Electronic Supplementary Information for

Grafting Challenging Monomers from Proteins using Aqueous ICAR ATRP under Bio-Relevant Conditions

Devora Cohen-Karni,[a,b] Marina Kovaliov,[a,b] Theresa Ramelot,[c] Dominik Konkolewicz,[c] Scott Graner,[d] and Saadyah Averick[a,b*]

[a]Neuroscience Disruptive Research Lab, Allegheny Health Network Research Institute, Allegheny General Hospital, Pittsburgh, Pennsylvania 15212, USA.

[b]Neuroscience Institute, Allegheny Health Network, Allegheny General Hospital, Pittsburgh, Pennsylvania 15212, USA.

[c]Department of Chemistry and Biochemistry, Miami University, Oxford, Ohio 45056, United States

[d]Department of Pathology Allegheny Health Network, Allegheny General Hospital, Pittsburgh, Pennsylvania 15212, USA

Materials. All reagents were used as received unless otherwise noted. Tris(2-pyridylmethyl)amine (TPMA), oligo(ethylene oxide) acrylate (M_n 475 g/mol, $OEOA_{475}$), acrylamide (AAm), *N,N*-dimethylacrylamide (DMA), *N*-vinylimidazole (VI), 1-Ethyl-3-(3-dimethylaminopropyl)carbodiimide (EDC·HCl), *N*-hydroxysuccinimide (NHS), 2-Bromo-2-methylpropionic acid, VA-044, Bovine serum albumin (BSA), were purchased from Sigma-Aldrich. Copper (II) bromide ($CuBr_2$) was purchased from Fisher Scientific. Water was deionized with a Millipore system as a Milli-Q grade. Monomers were passed over a column of basic alumina prior to use to remove the inhibitor. 10×PBS was purchased from Corning and diluted as indicated. (1×PBS = 2 mg/mL KCl , 2 mg/mL KH_2PO_4, 80 mg/mL NaCL, 11.5 mg/mL $Na_2HPO)_4$. Sodium dodecyl sulfate poly(acrylamide) gel electrophoresis (SDS-PAGE) Mini-PROTEAN TGX 4−20% (gradient) and Bio-safe Coomassie G-250 stain were purchased from Bio-Rad, and used for all SDS-PAGE. 10X Tris-Glycine SDS buffer was purchased from Thermo-scientific, 3×SDS blue loading buffer was purchased from New-England Biolabs and Full Range Rainbow Molecular Weight marker was purchased from GE Healthcare Life Sciences and used in all SDS-PAGE.

Instrumentation. Aqueous GPC was performed on an Agilent GPC system equipped with a refractive index and diode array detector. An 1260 Infinity Isocratic Pump and an Agilent Bio SEC-3 column was used with running buffer of 100 mM sodium phosphate with 0.2 vol% trifluoroacetic acid (pH = 2.5) at a flow rate of 1 ml per min. Linear poly(ethylene oxide) (M_n = 1,400 – 389,500) standards was used for the calibration of the system. UV-vis absorbance spectra were collected on a NanoDrop 2000c spectrophotometer. Monomer conversion was measured using ^{1}H NMR in D_2O, using a Bruker Avance 500 MHz spectrometer. MALDI-TOF data acquisition was performed on a Bruker AutoFlexIII MALDI-TOF mass spectrometer at Miami University. BSA and polymer-conjugated samples were used at 1 mg/mL concentrations. All samples were mixed with the appropriate matrix (sinapinic acid (SA) and α-cyano-4-hydroxycinnamic (CCA) in a 1:1 (v/v) ratio before spotting on the MALDI plate. Mass spectra were calibrated using BSA (66.4 m/z) as an external standard. In general, 3.0 μL of sample (1 mg/mL) was mixed with 3.0 μL of saturated SA solution (0.1% TFA, 40% acetonitrile) and 1 μL

was spotted directly on the target plate and allowed to dry at room temperature. Alternatively, a two-layer method was used where the bottom layer was 1 μL of a 10 mg/ml solution of CCA in acetone spotted and dried on the plate. A second layer of 1 μL sample was spotted on top of the first layer and allowed to dry. This was made by mixing 3 μL of sample with 3.0 μL of saturated CCA solution (0.1% TFA, 40% acetonitrile). Data was collected positive ion linear mode to detect $[M+H]^+$ ions and analyzed by Bruker Daltonics flexAnalysis software. TEM images were taken using 10 μL of biohybrid that was deposited onto a carbon coated grid and subsequently blotted off. The sample was imaged on a Philips CM10 Electron Microscope (60 kV) with images recorded on film. For SEM images, the biohybrid sample was re-suspended in 200uL isopropyl alcohol and then drop casted onto 5mm by 5mm SI/600nm wet thermal oxide substrate. The sample was images in FEI Quanta 600, with acceleration voltage of 2-20 kV and working distance of 10mm. RP-HPLC spectra were collected using an 1260 Infinity Isocratic Pump with an ZirChrom®-PBD column (50 mm x 2.1 mm i.d., 3 micron). The mobile phase was acetonitrile/10 mM ammonium acetate (v/v = 45/55) with 0.1 mM citrate (pH 4.4) and the temperature was 25 °C. The flow rate was set at 0.3 ml/min. Samples were analyzed by ESI-MS on a LCQ (Thermo Scientific, San Jose, CA) mass spectrometer operated using flow injection analysis (FIA) for sample introduction.

Methods

Synthesis of BSA-[*i*BBr]$_{10}$. 2-Bromo-2-methylpropionic acid (715.7 mg, 4.3 mmol) was dissolved in 85 ml of 1×PBS (2.7 mM KCl, 140 mM NaCl, 1.5 mM KH_2PO_4, 8.1 mM Na_2HPO_4), with EDC (818 mg, 4.3 mmol) and sulfo-NHS (186.7 mg, 0.86 mmol). BSA (1.0 g, 0.43 mmol Lys) was dissolved in 15 ml of 1×PBS (pH 7.4). The first was injected (1 mL/min) into the protein solution. The reaction was stirred for 3 hrs and purified by dialysis with a 30-kDa molecular weight cut off membrane against 1×PBS, followed by filtration with 0.8 μM PES filters to remove precipitation.

ICAR ATRP from BSA-[*i*BBr]$_{10}$. BSA-[iBBr]$_{10}$ (33.0 mg (protein), 0.5 μmol (4.2 μmol initiator)), monomer (as indicated) (5.6 mmol), $CuBr_2$ (1.25, 0.0056 mmol), TPMA (4.06 mg, 0.014 mmol) and VA-044 (3.62 mg, 0.011 mmol) were dissolved in 10 ml of indicated solvent (PBS or water) and charged into a 25 ml Schlenk flask. 0.2 ml of DMF was added as internal

standard for ^{1}H NMR measurement of monomer conversion. The reaction mixture was purged with N_2 for 20 minutes then placed in a water bath at 44 ^{o}C.

ICAR ATRP from BSA-polymer: BSA-polymer-Br (12 mg (protein), 0.2 μmol (1.5 μmol initiator)), monomer (as indicated) (2.8 mmol), $CuBr_2$ (0.63 mg, 0.0028 mmol), TPMA (2.03 mg, 0.007 mmol) and VA-044 (1.81 mg, 0.056 mmol) were dissolved in 5ml of indicated solvent (PBS or water) and charged into a 10 ml Schlenk flask. 0.2 ml of DMF was added as internal standard for ^{1}H NMR measurement of monomer conversion.. The reaction mixture was purged with N_2 for 20 minutes then placed in a water bath at 44 ^{o}C.

Preparation of BSA-poly(Pd-VI)-*b*-poly(OEOA). To a yellowish solution of **BSA-poly(VI)-*b*-poly(OEOA)** biohybrid (13.2 mg, 0.01 mmol imidazole) in methanol (0.5 mL) was slowly added an aqueous solution of $(NH_4)_2PdCl_4$ (10 mg, 0.05 mmol; 0.5 mL) at 25 °C. The resulting brown suspension was heated at 60 °C for 30 min. The brown solution was centrifuged to obtain brown precipitates. The precipitates were washed with H_2O and MeOH and the solid recovered by centrifugation separation. The precipitates were dried under reduced pressure to give the desired catalyst (10 mg, 75% mass recovery).

General Procedure for Suzuki–Miyaura Coupling. A glass 2.5 mL vessel was charged with appropriate bromide (0.25 mmol), pheylboronic acid (0.6 mmol), BSA-poly(Pd-VI)-b-poly(OEOA) (3.75 mg, 2.5×10^{-5} mmol, 0.01 mol %), K_2CO_3 (0.5 mmol), TBAF (0.5 mmol), and H_2O (1.5 mL). The mixture was stirred at 100 °C for 24 h. The reaction mixture was cold at room temperature and diluted with EtOAc and H_2O. The organic layer was separated and the aqueous layer was extracted with EtOAc. The combined organic layers were dried over MgSO4, and concentrated under reduced pressure. The crude product was analyzed by RP-HPLC and MS.

Biphenyl-fentanyl **(3).** Yield 55%; MS (*m/z*): 4-bromo-fentanyl**, 1:** $[M+H]^+$ $C_{22}H_{28}BrN_2O$ 415.487; **3**: $[M+H]^+$ $C_{28}H_{33}N_2O$ 413.460

1,1'-Biphenyl-4-yl(phenyl)methanol **(5)**. Yield 80%**;** MS (*m/z*): 4-bromobenzhydrol, **4:** $[M-H]^-$ $C_{13}H_{10}BrO$ 260.233; **5**: $[M-H]^-$ $C_{19}H_{15}O$ 259.289

General Procedure for Control Suzuki–Miyaura Coupling. A glass 2.5 mL vessel was charged with appropriate bromide (0.25 mmol), pheylboronic acid (0.6 mmol), BSA-poly(VI)-b-poly(OEOA) (3.75 mg, 2.5×10^{-5} mmol, 0.01 mol %) **or** $(NH_4)_2PdCl_4$ (0.71 mg, 2.5×10^{-3} mmol, 0.01 mol %), K_2CO_3 (0.5 mmol), TBAF (0.5 mmol), and H_2O (1.5 mL). The mixture was stirred at 100 °C for 24 h. The reaction mixture was cold at room temperature and diluted with EtOAc and H_2O. The organic layer was separated and the aqueous layer was extracted with EtOAc. The combined organic layers were dried over MgSO4, and concentrated under reduced pressure. The crude product was analyzed by RP-HPLC.

BSA-poly(VI)-b-poly(OEOA) control: no product was detected by RP-HPLC

$(NH_4)_2PdCl_4$ control: Biphenyl-fentanyl **(3)**: Yield 26%; 1,1'-Biphenyl-4-yl(phenyl)methanol **(5)**: Yield 57%**.**

MALDI-TOF MS data

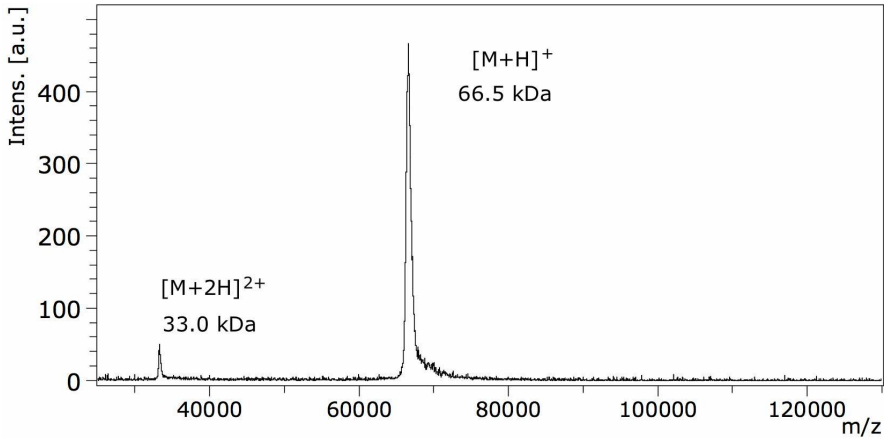

Figure S1. MALDI-TOF MS data for the pure BSA (m/z 66.5 kDa).

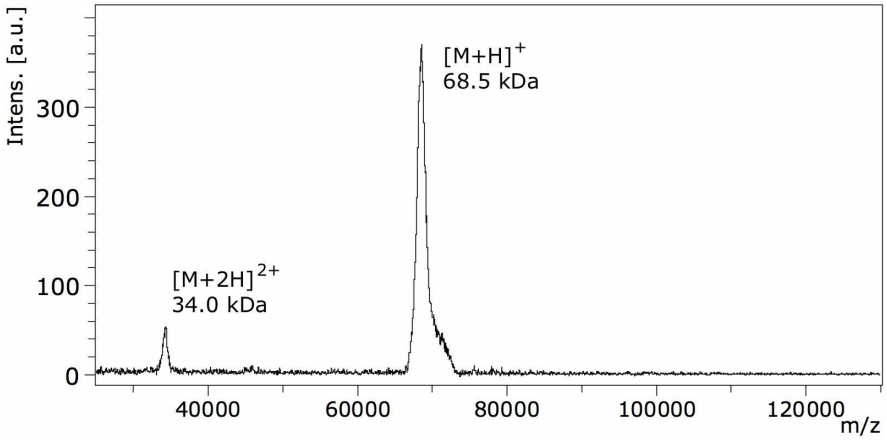

Figure S2. MALDI-TOF MS data for the BSA-*i*BBr (m/z 68.5 kDa).

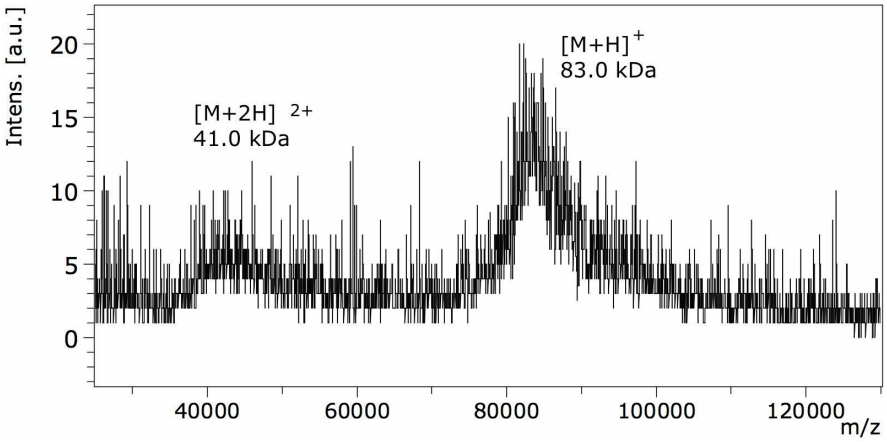

Figure S3. MALDI-TOF MS data for BSA-poly(OEOA) (m/z 83 kDa).

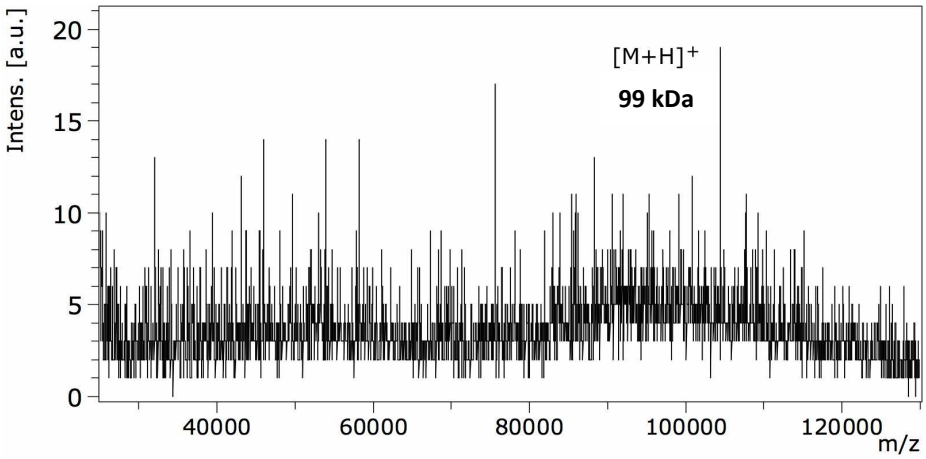

Figure S4. MALDI-TOF MS data for BSA-poly(AAm) (m/z 99 kDa).

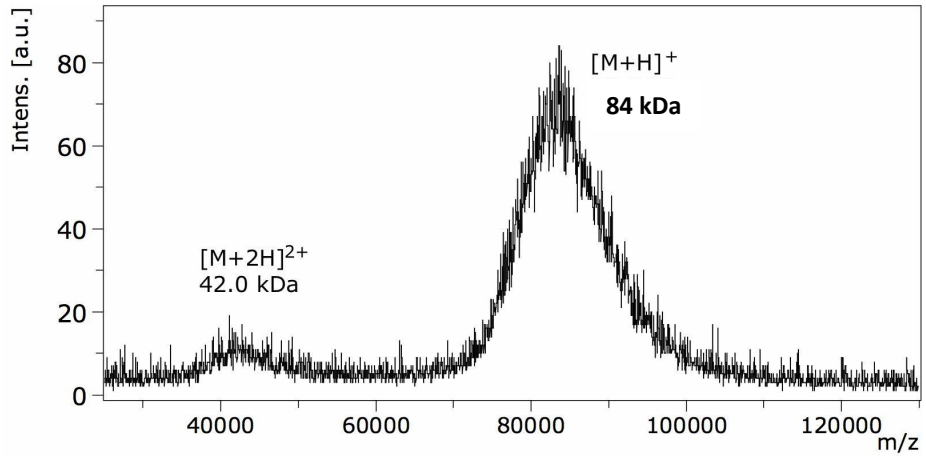

Figure S5. MALDI-TOF MS data for BSA-poly(DMA) (m/z 84 kDa).

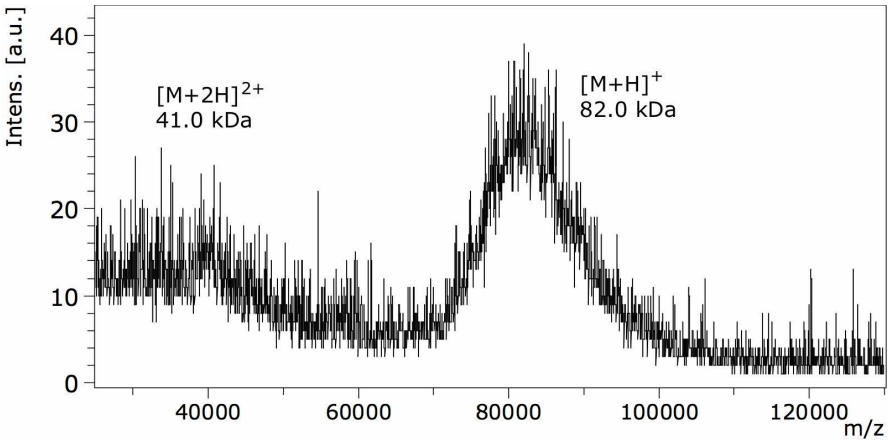

Figure S6. MALDI-TOF MS data for BSA-poly(VI) (m/z 82 kDa).

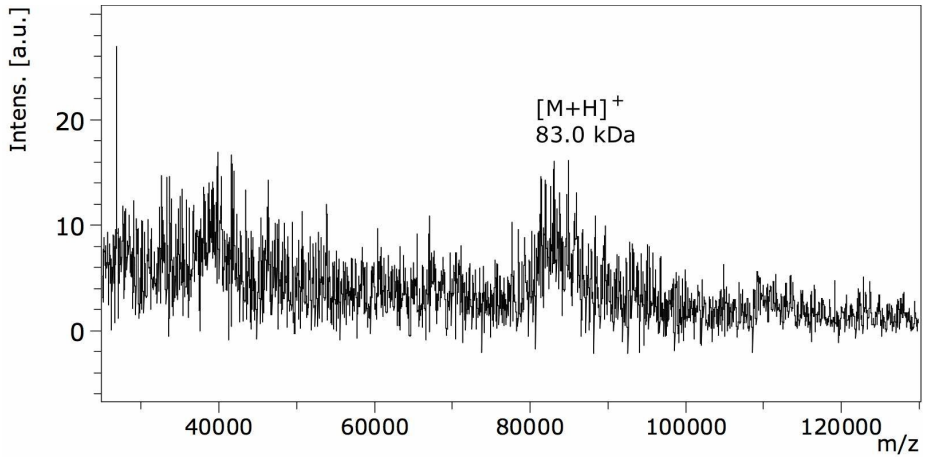

Figure S7. MALDI-TOF MS data for BSA-poly(DMA) (m/z 83 kDa).

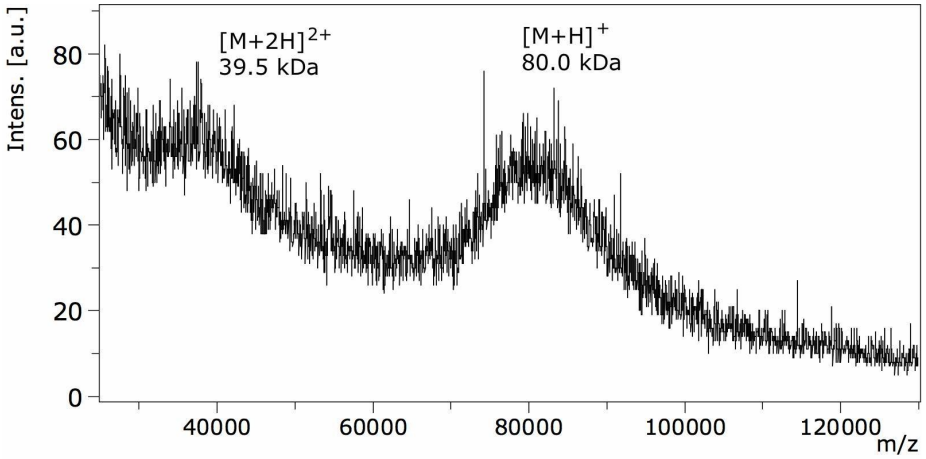

Figure S8. MALDI-TOF MS data for BSA-poly(VI) (m/z 80 kDa).

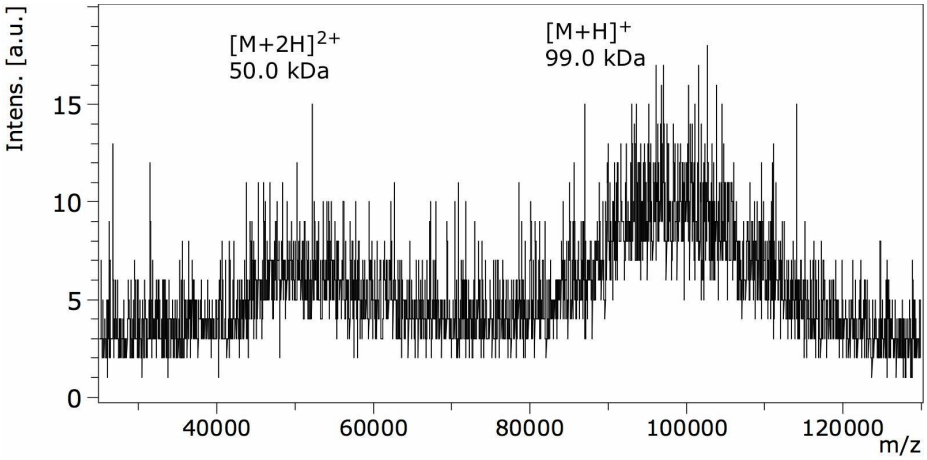

Figure S9. MALDI-TOF MS data for BSA-poly(OEOA)-*b*-poly(DMA) (m/z 99 kDa).

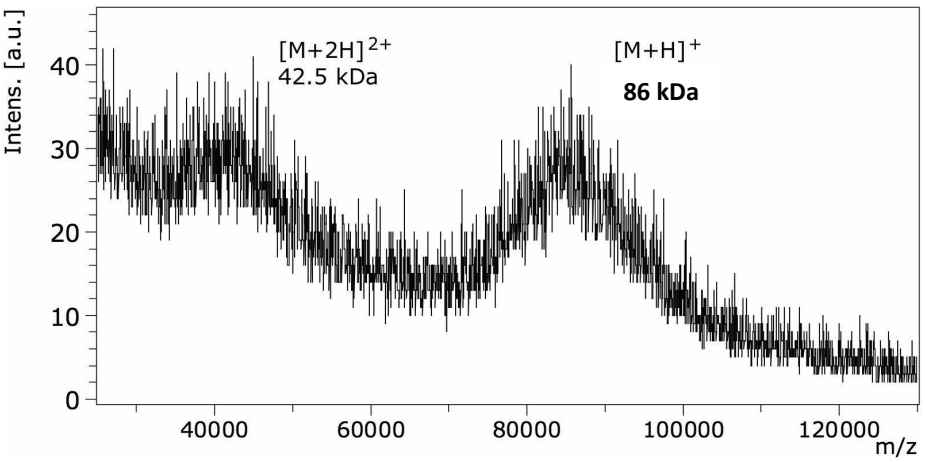

Figure S10. MALDI-TOF MS data for BSA-poly(DMA)-*b*-poly(AAm) (m/z 86 kDa).

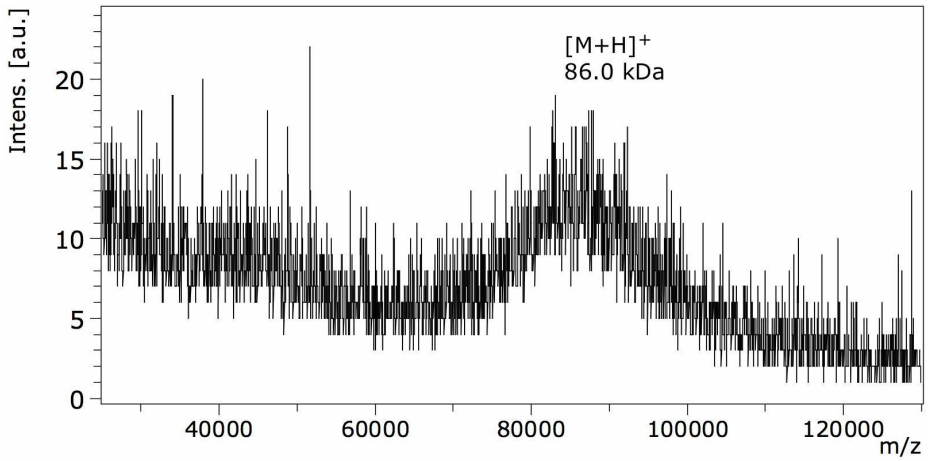

Figure S11. MALDI-TOF MS data for BSA-poly(VI)-*b*-poly(AAm) (m/z 86 kDa).

SDS-PAGE

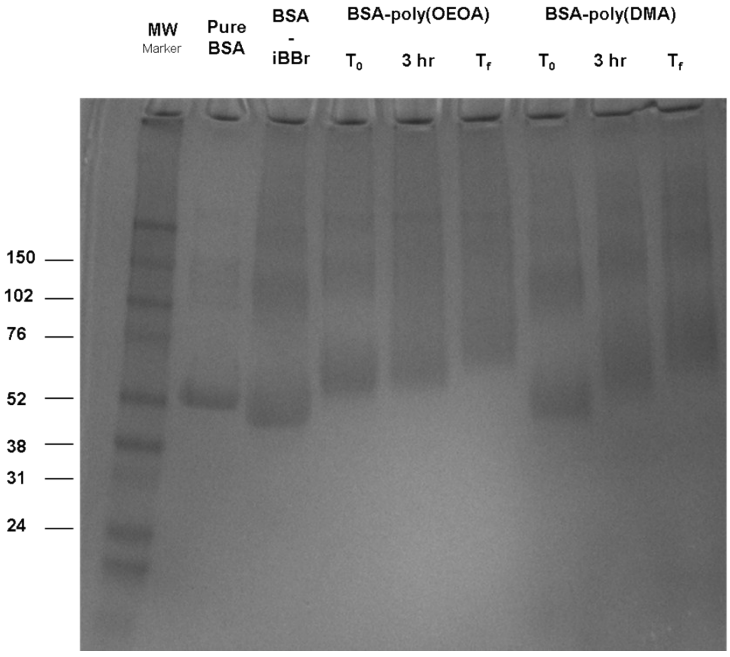

Figure S12. Progress of ATRP reaction monitored by SDS-PAGE of BSA-poly(OEOA) and BSA-poly(DMA).

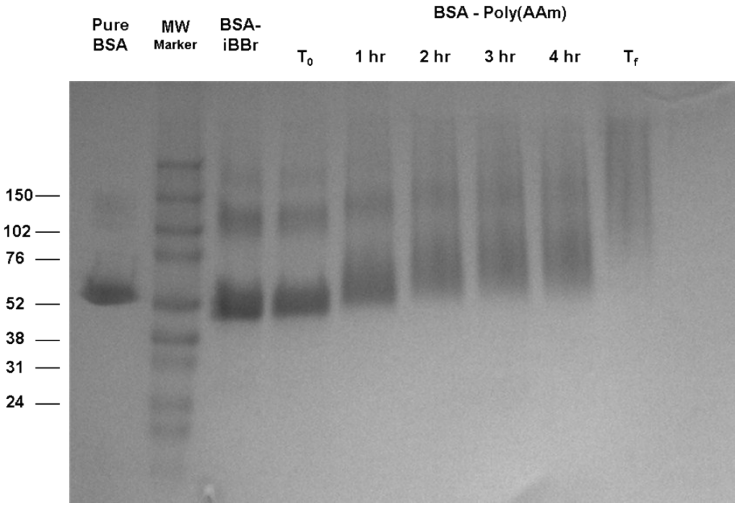

Figure S13. Progress of ATRP reaction monitored by SDS-PAGE of BSA-poly(AAm).

HPLC Traces for Suzuki-Miyaura reactions with poly(Pd-VI)-*b*-poly(OEOA) hybrid

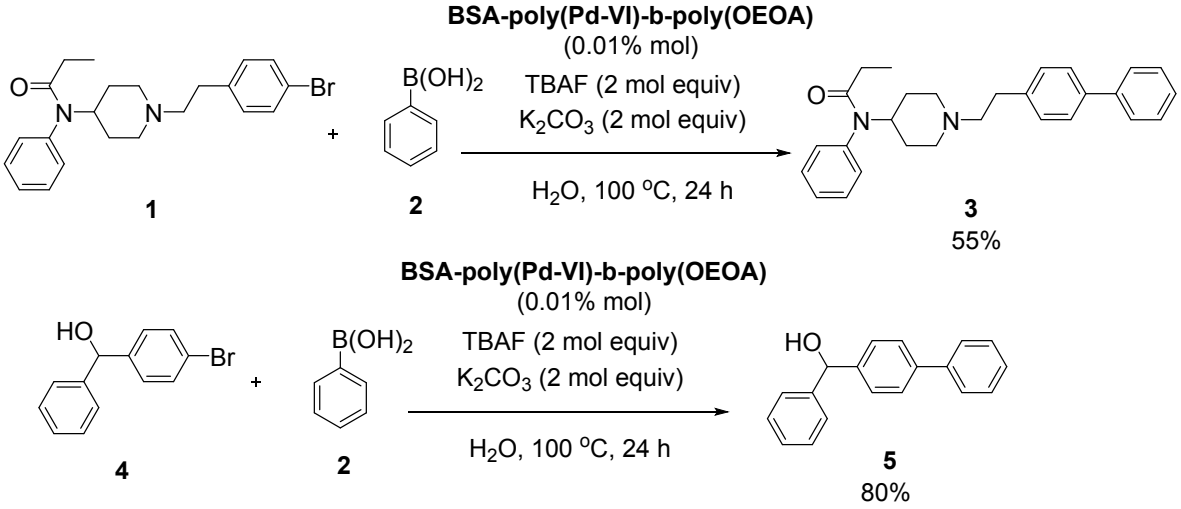

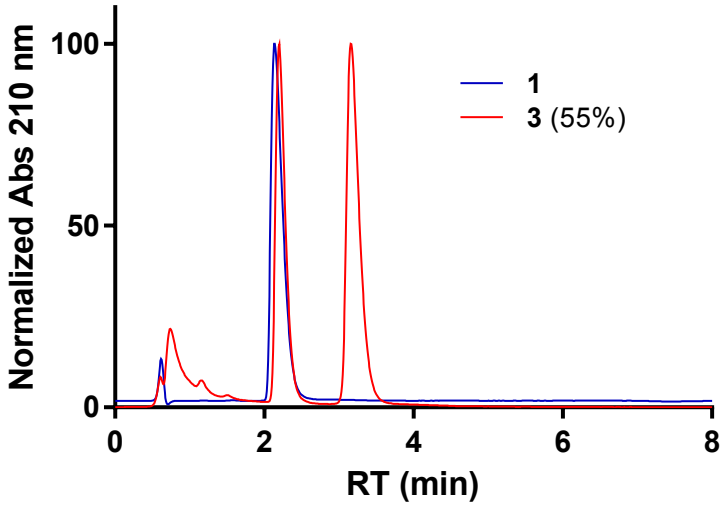

Figure S14. HPLC traces of 4-bromo-fentanyl, **1** (blue) and the crude product biphenyl-fentanyl, **3** (red).

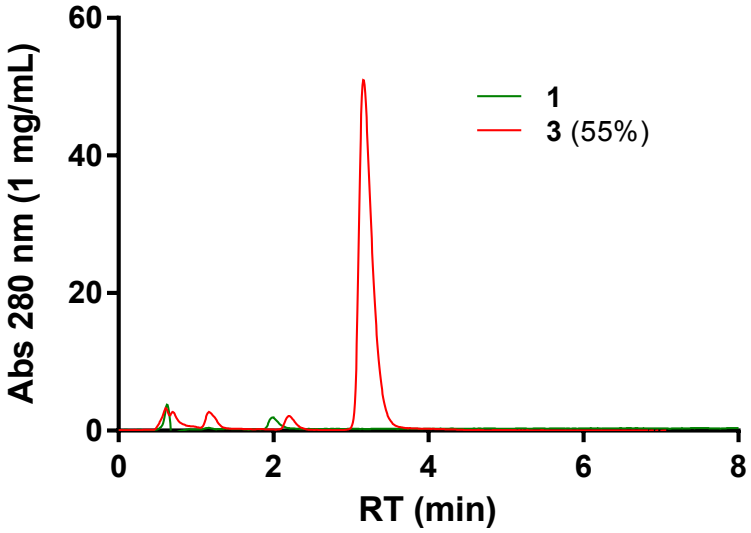

Figure S15. HPLC traces of 4-bromo-fentanyl, **1** (green) and the crude product biphenyl-fentanyl, **3** (red).

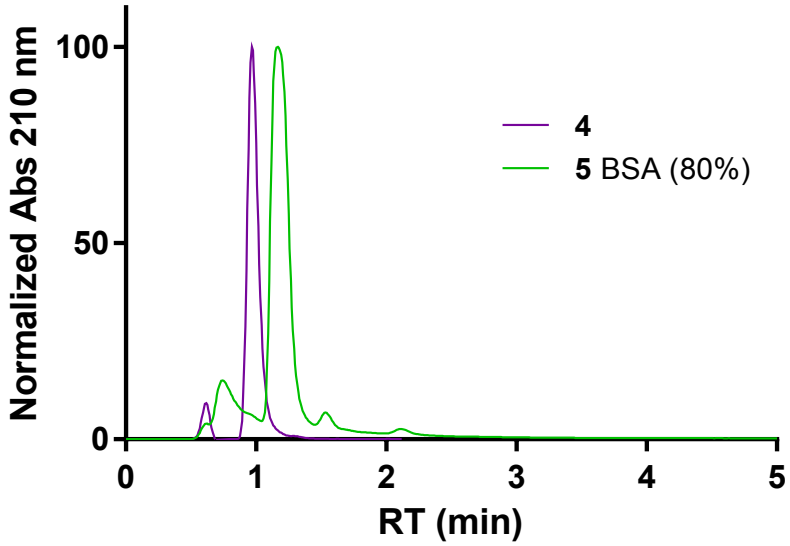

Figure S16. HPLC traces of 4-bromobenzhydrol, **4** (purple) and the crude product 1'-biphenyl-4-yl(phenyl)methanol, **5** (green).

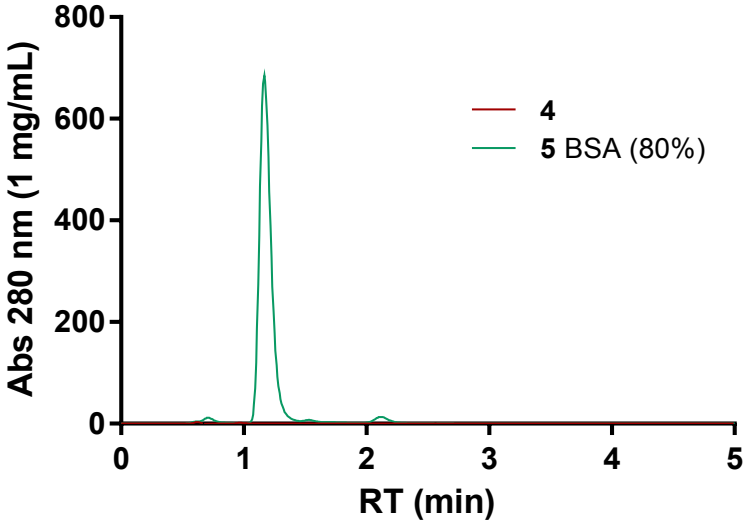

Figure S17. HPLC traces of 4-bromobenzhydrol, **4** (red) and the crude product 1'-biphenyl-4-yl(phenyl)methanol, **5** (green).

HPLC Traces for Control Suzuki-Miyaura Reactions with poly(VI)-*b*-poly(OEOA) hybrid

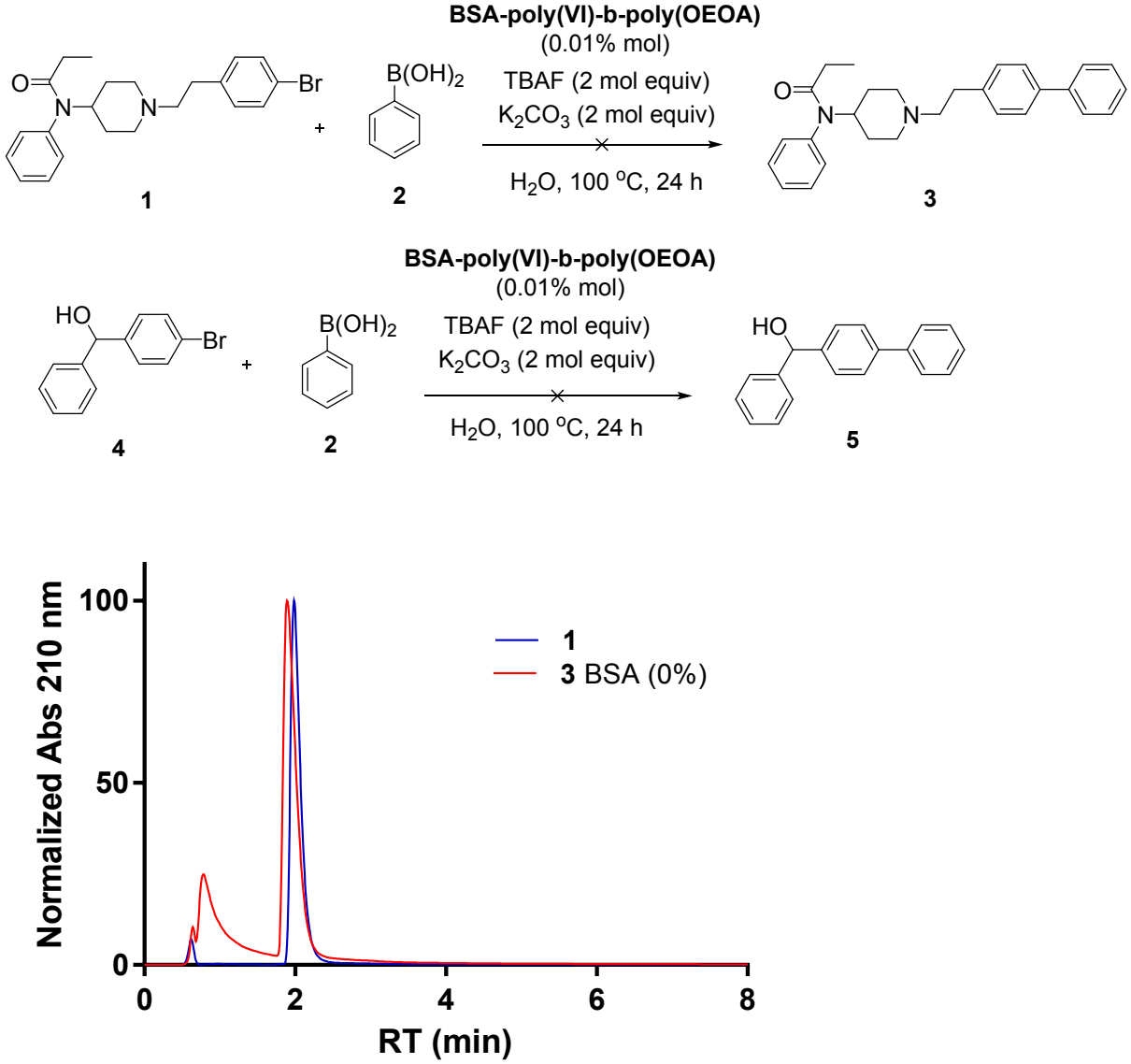

Figure S18. HPLC traces of 4-bromo-fentanyl, **1** (blue) and the crude product biphenyl-fentanyl, **3** (red).

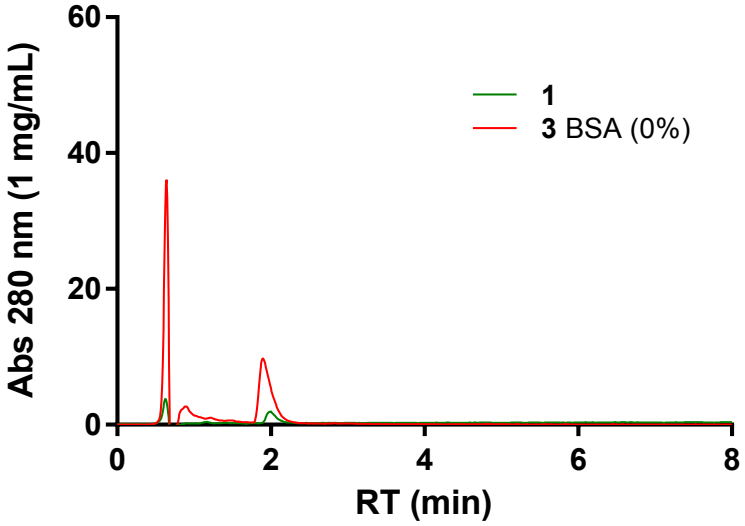

Figure S19. HPLC traces of 4-bromo-fentanyl, **1** (green) and the crude product biphenyl-fentanyl, **3** (red).

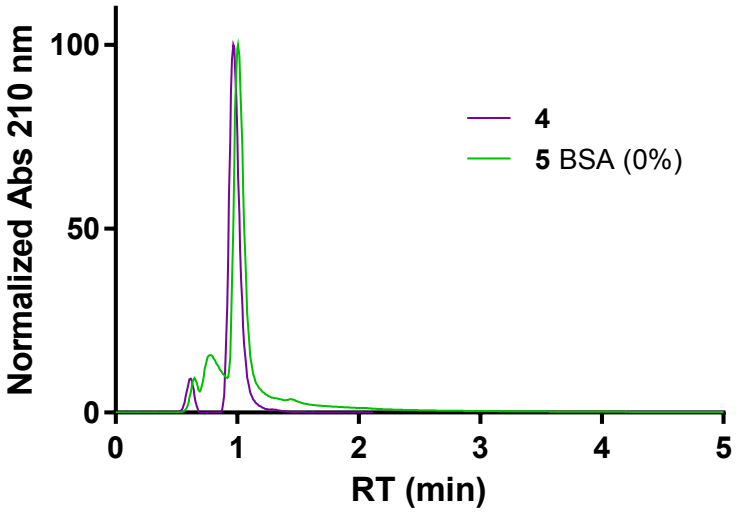

Figure S20. HPLC traces of 4-bromobenzhydrol, **4** (purple) and the crude product 1'-biphenyl-4-yl(phenyl)methanol, **5** (green).

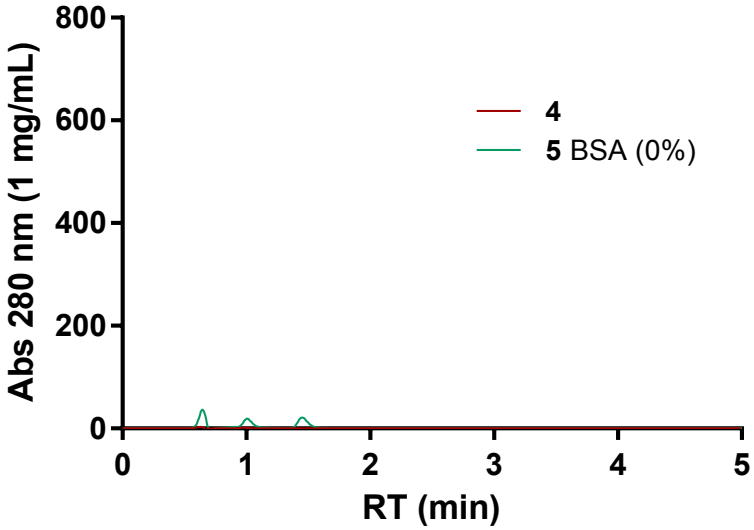

Figure S21. HPLC traces of 4-bromobenzhydrol, **4** (red) and the crude product 1'-biphenyl-4-yl(phenyl)methanol, **5** (green).

HPLC Traces for Control Suzuki-Miyaura Reactions with $(NH_4)_2PdCl_4$

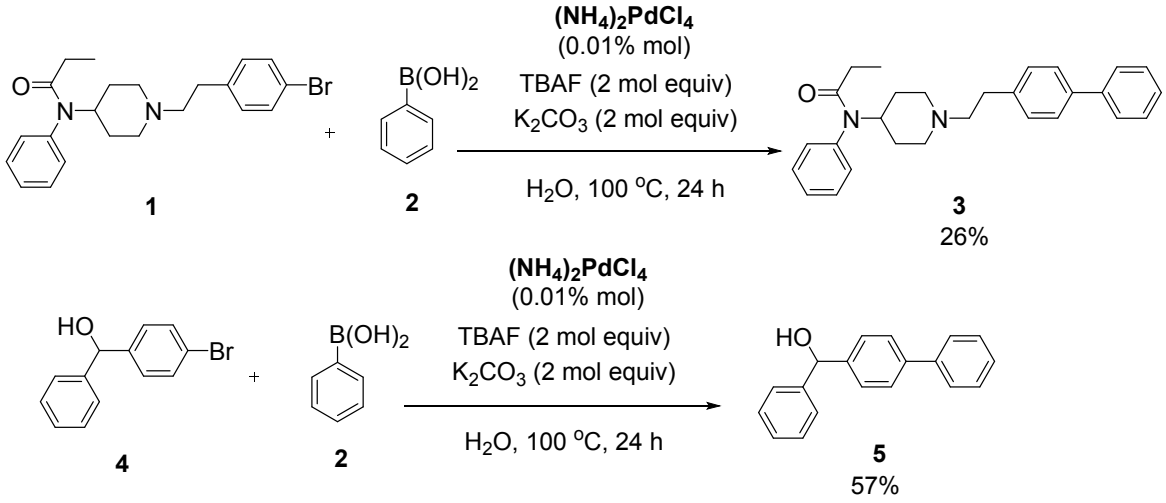

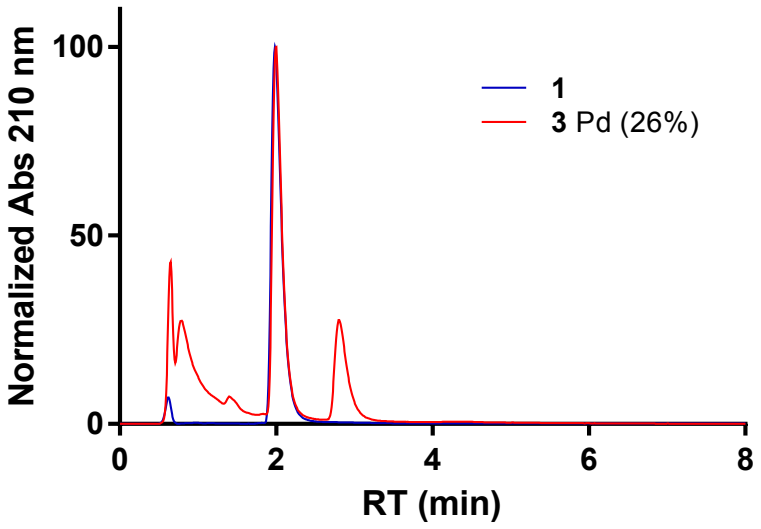

Figure S22. HPLC traces of 4-bromo-fentanyl, **1** (blue) and the crude product biphenyl-fentanyl, **3** (red).

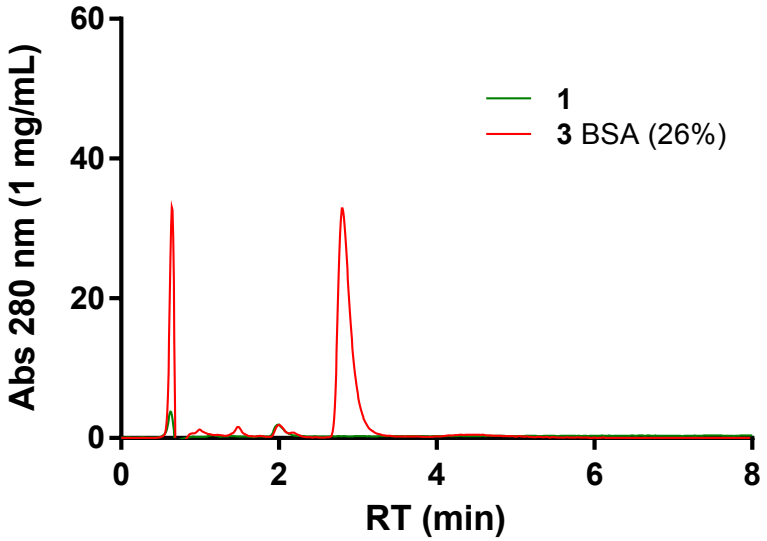

Figure S23. HPLC traces of 4-bromo-fentanyl, **1** (green) and the crude product biphenyl-fentanyl, **3** (red).

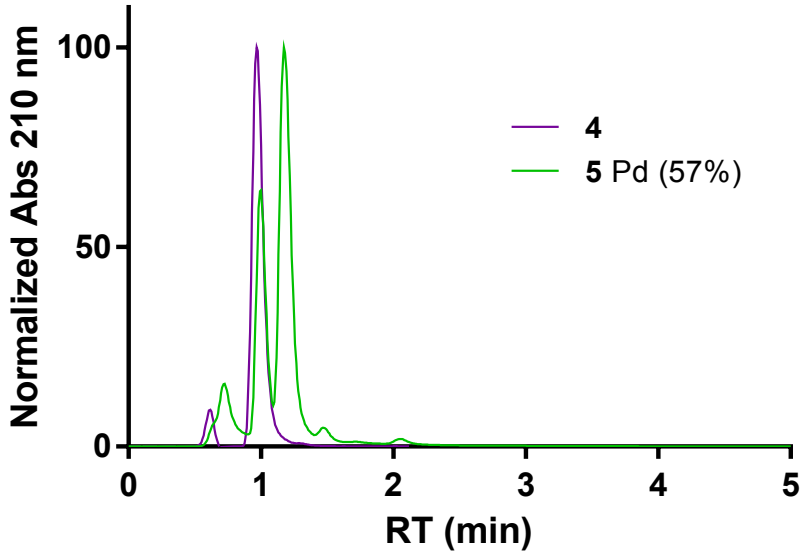

Figure S24. HPLC traces of 4-bromobenzhydrol, **4** (purple) and the crude product 1'-biphenyl-4-yl(phenyl)methanol, **5** (green).

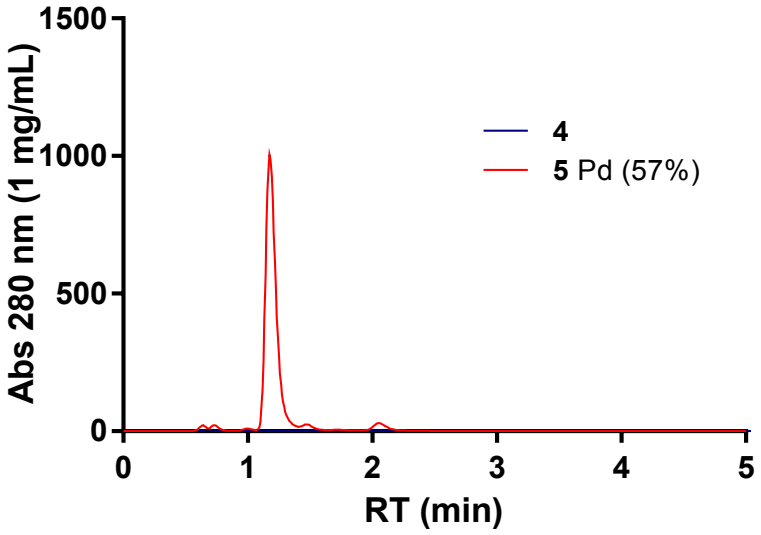

Figure S25. HPLC traces of 4-bromobenzhydrol, **4** (blue) and the crude product 1'-biphenyl-4-yl(phenyl)methanol, **5** (red).

ESI-MS data for Suzuki-Miyaura reactions with poly(Pd-VI)-*b*-poly(OEOA).

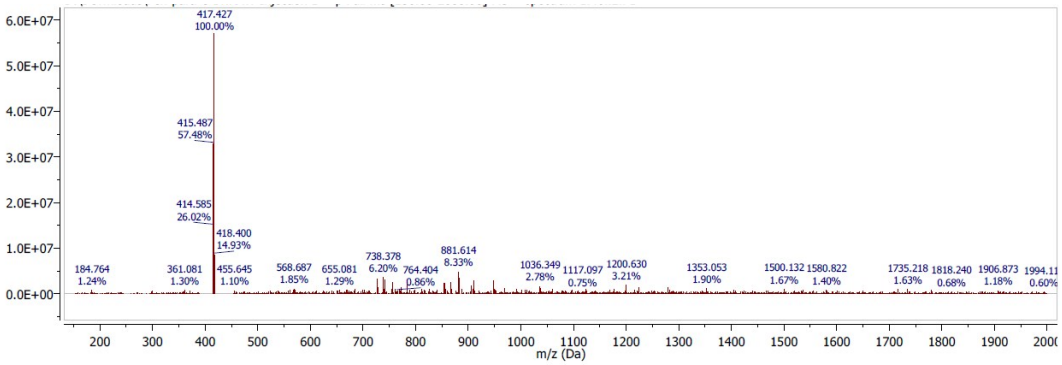

Figure S26. MS data for 4-bromo-fentanyl, **1**.

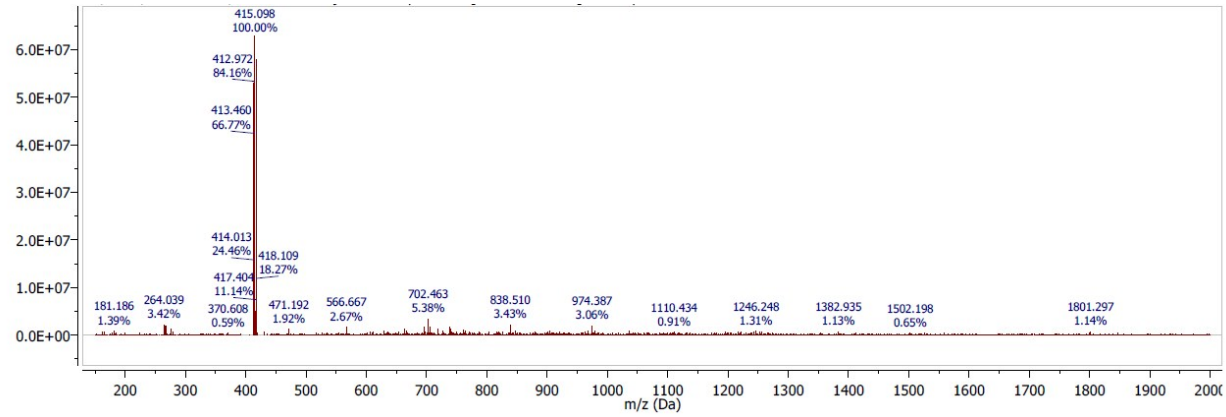

Figure S27. MS data for biphenyl-fentanyl, **3**.

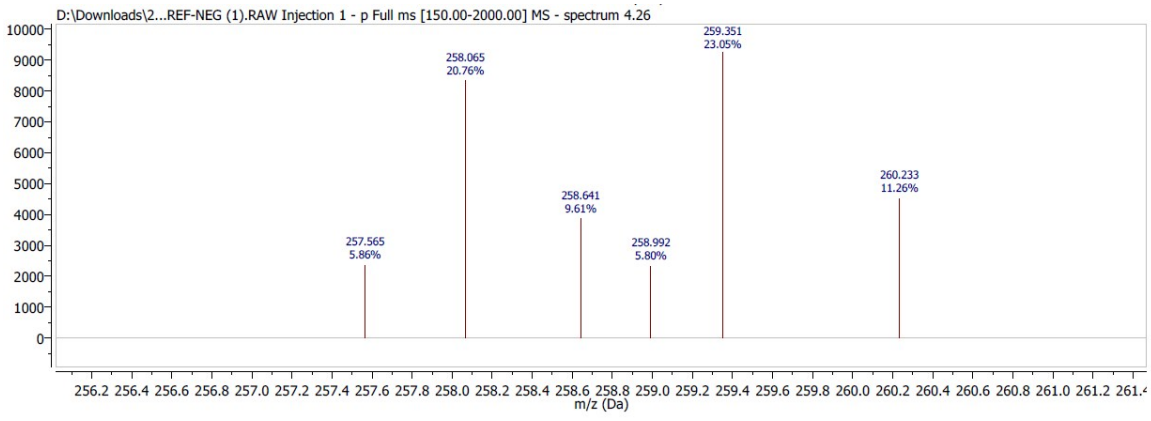

Figure S28. MS data for 4-bromobenzhydrol, **4**.

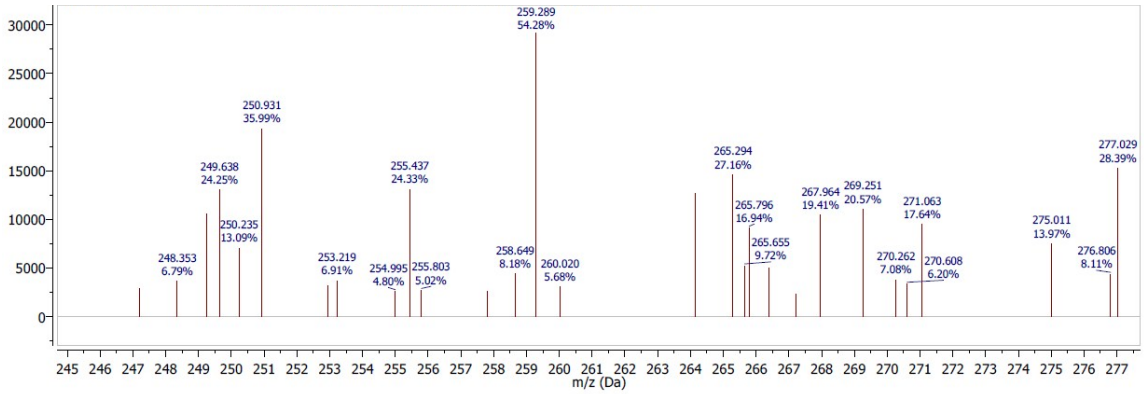

Figure S29. MS data for 1'-biphenyl-4-yl(phenyl)methanol, **5**.

TEM images

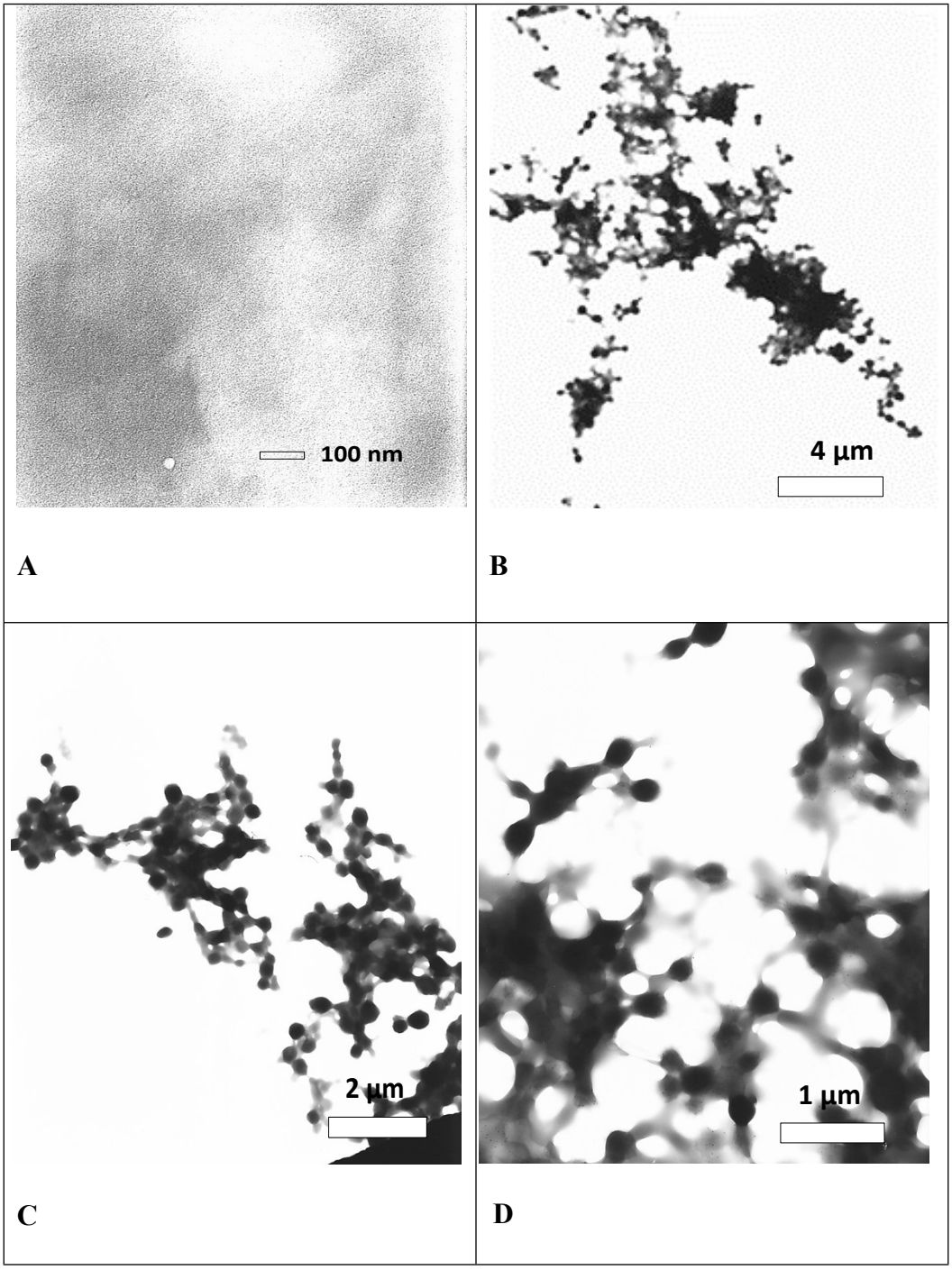

Figure S30. (60 kV) TEM micrographs of BSA-pVI-*b*-pOEOA before (A) and after (B), (C), (D) Pd loading at increasing magnification

SEM images

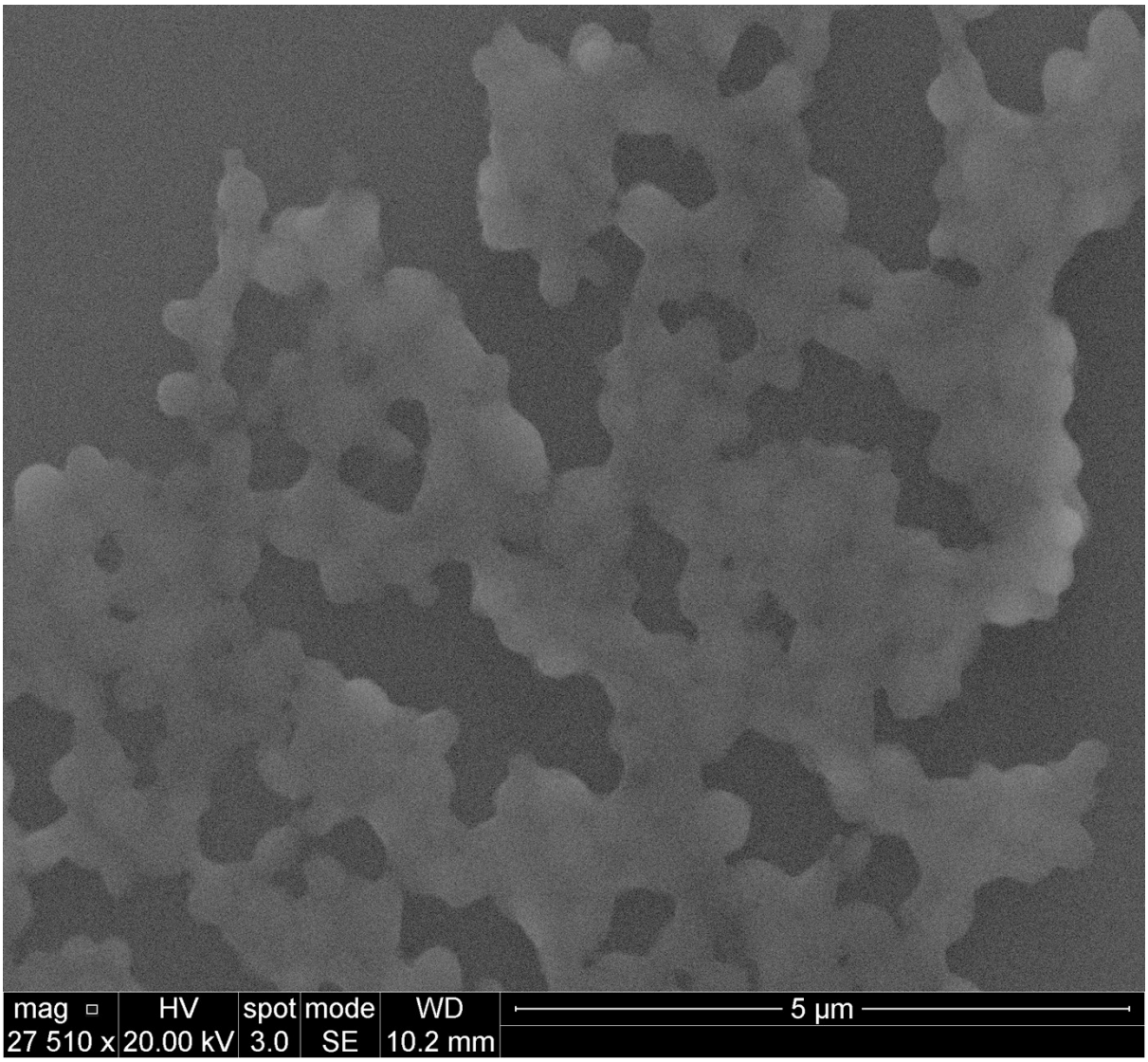

Figure S31. SEM image micrographs of BSA-pVI-*b*-pOEOA after Pd loading.

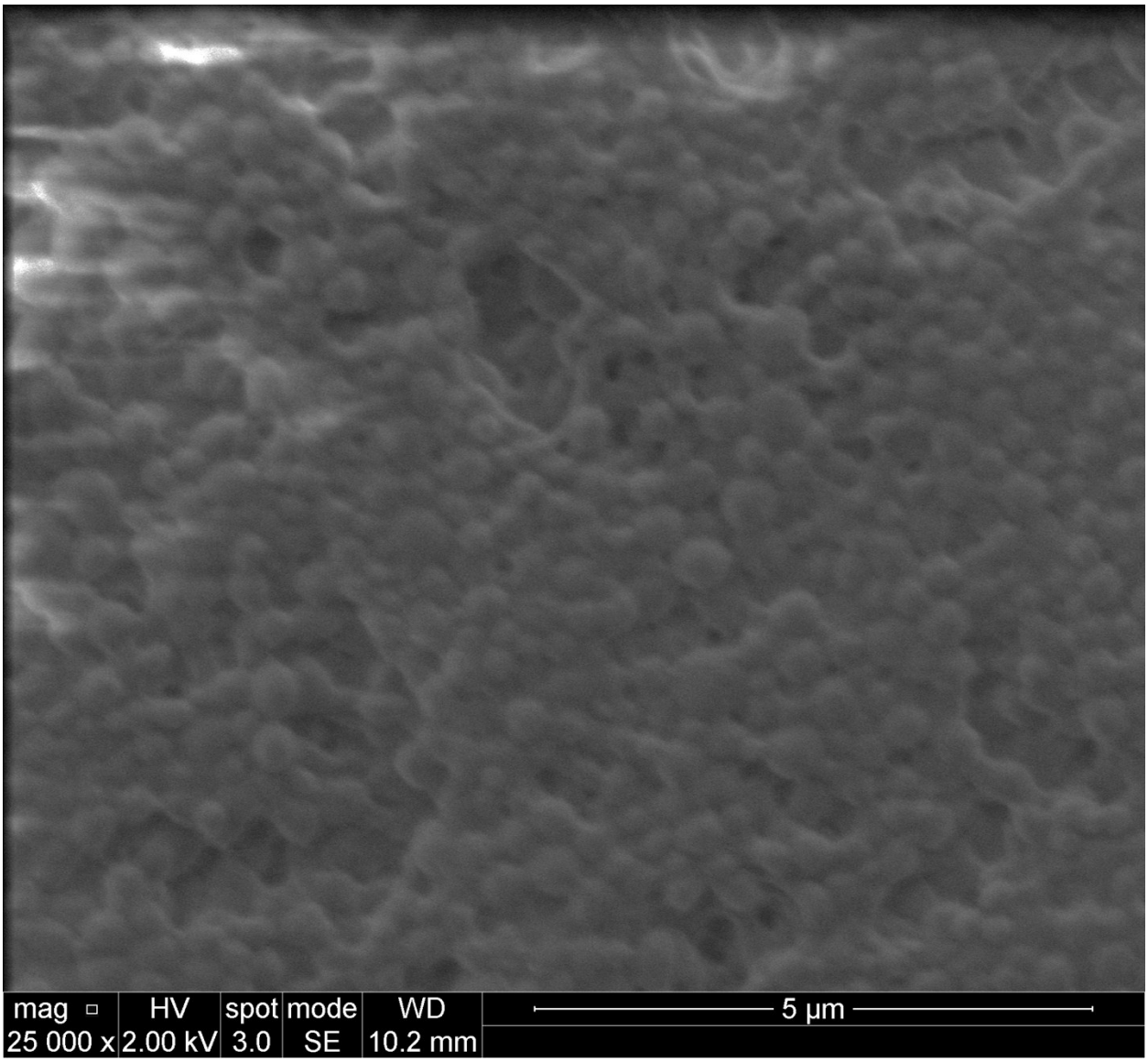

Figure S32. SEM image micrographs of BSA-pVI-*b*-pOEOA after Pd loading.

EDS Analysis on the SEM

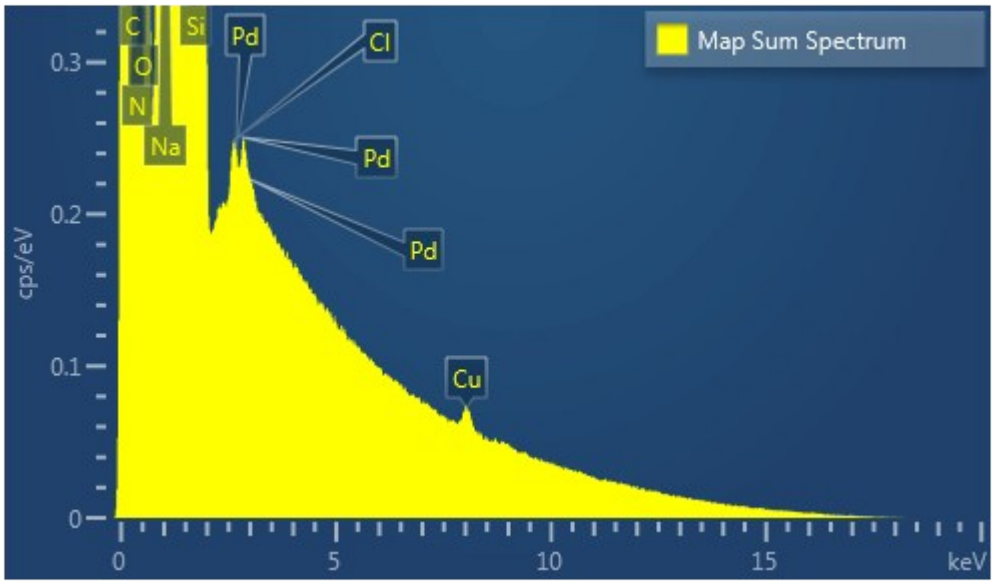

Figure S33. EDS SEM image micrographs of BSA-pVI-*b*-pOEOA after Pd loading.

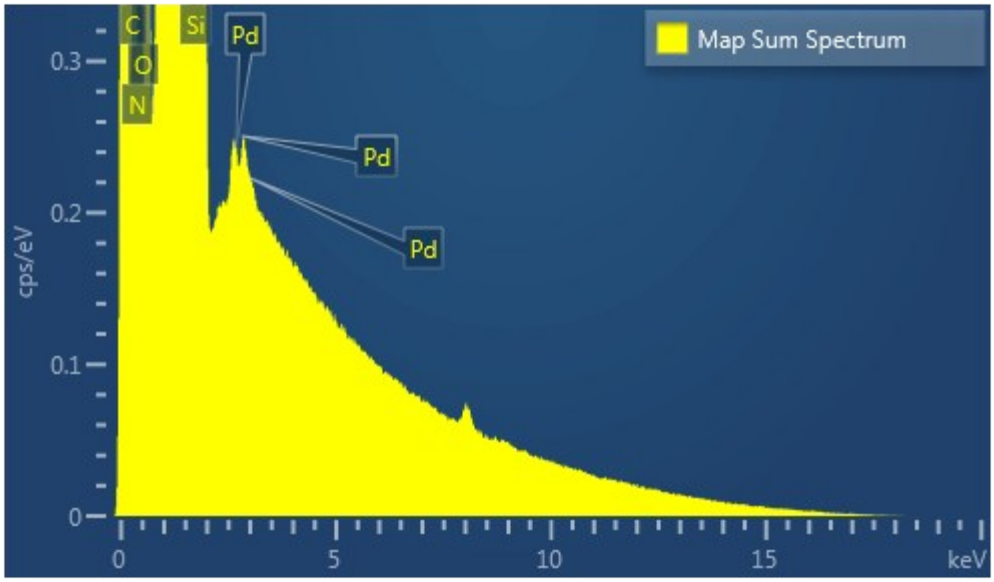

Figure S34. EDSSEM image micrographs of BSA-pVI-*b*-pOEOA after Pd loading.